Gene Duplication in the Diversification of Secondary Metabolism: Tandem 2-Oxoglutarate–Dependent Dioxygenases Control Glucosinolate Biosynthesis in Arabidopsis

Daniel J. Kliebenstein, Virginia M. Lambrix, Michael Reichelt, Jonathan Gershenzon, and Thomas Mitchell-Olds[1]

Max Planck Institute for Chemical Ecology, 07745 Jena, Germany

Secondary metabolites are a diverse set of plant compounds believed to have numerous functions in plant–environment interactions. The large chemical diversity of secondary metabolites undoubtedly arises from an equally diverse set of enzymes responsible for their biosynthesis. However, little is known about the evolution of enzymes involved in secondary metabolism. We are studying the biosynthesis of glucosinolates, a large group of secondary metabolites, in Arabidopsis to investigate the evolution of enzymes involved in secondary metabolism. Arabidopsis contains natural variations in the presence of methylsulfinylalkyl, alkenyl, and hydroxyalkyl glucosinolates. In this article, we report the identification of genes encoding two 2-oxoglutarate–dependent dioxygenases that are responsible for this variation. These genes, *AOP2* and *AOP3*, which map to the same position on chromosome IV, result from an apparent gene duplication and control the conversion of methylsulfinylalkyl glucosinolate to either the alkenyl or the hydroxyalkyl form. By heterologous expression in Escherichia and the correlation of gene expression patterns to the glucosinolate phenotype, we show that *AOP2* catalyzes the conversion of methylsulfinylalkyl glucosinolates to alkenyl glucosinolates. Conversely, *AOP3* directs the formation of hydroxyalkyl glucosinolates from methylsulfinylalkyl glucosinolates. No ecotype coexpressed both genes. Furthermore, the absence of functional *AOP2* and *AOP3* leads to the accumulation of the precursor methylsulfinylalkyl glucosinolates. A third member of this gene family, *AOP1*, is present in at least two forms and found in all ecotypes examined. However, its catalytic role is still uncertain.

INTRODUCTION

The sessile nature of plants forces them to cope directly with environmental stresses, which include insect herbivory, pathogen attack, UV light radiation, and drought. Secondary metabolites are believed to be an important mechanism that allows plants to respond to these environmental challenges. There are more than 100,000 known plant secondary metabolites, which probably represent less than 10% of the actual total in nature (Wink, 1988). A large fraction of this diversity is derived from differential modification of common backbone structures, which requires the evolution of numerous enzymes with different product specificities. There are several mechanisms by which this can occur. First, as is the case with terpene synthases, a single protein can produce numerous products from a single substrate (Steele et al., 1998). A few amino acid substitutions can alter the ratio of products generated by a terpene synthase (Back and Chappell,

1996). The second mechanism is the use of gene duplication. In this model, a gene encoding an enzyme is duplicated, allowing one copy to evolve a new product profile while the other copy maintains its original function (Lynch and Force, 2000). To examine the mechanisms responsible for the evolution of diversity in plant secondary metabolites, we are studying glucosinolate biosynthesis in Arabidopsis.

The largest known group of secondary metabolites in Arabidopsis is the glucosinolates, with more than 30 different structures described (Hogge et al., 1988; D. Kliebenstein and T. Mitchell-Olds, unpublished data). In Arabidopsis, glucosinolates are biosynthesized from a variety of typical protein amino acids (methionine, tryptophan, and phenylalanine) and their chain-elongated analogs. The first step in glucosinolate biosynthesis is the oxidation of the amino group to an oxime moiety by amino acid–specific cytochrome P450 monooxygenases (Du et al., 1995; Wittstock and Halkier, 2000). After a thiohydroximate intermediate is formed, sequential transfer of glucose and sulfate residues creates the basic glucosinolate skeleton (Halkier and Du, 1997). The initially formed glucosinolate can undergo a variety of subsequent

[1] To whom correspondence should be addressed. E-mail tmo@ice.mpg.de; fax 49-3641-643668.

transformations that modify the side chain. For example, the C_4 dihomomethionine-derived glucosinolate backbone can be modified into seven different glucosinolates in Arabidopsis (Figure 1). Because most of these modifications are sequential, each step probably is catalyzed by a different enzyme that likely had to evolve independently.

When tissue disruption brings the glucosinolate into contact with myrosinase, a thioglucosidase, numerous compounds (isothiocyanates, nitriles, epithiocyanates, and thiocyanates) with diverse biological activities are formed. The glucosinolates and their derivatives can act as feeding deterrents or attractants for different insect species (Giamoustaris and Mithen, 1995). In addition, they can have nutritional effects that range from being goitrogenic to potential anticarcinogens (Faulkner et al., 1998). This assortment of biological activities associated with glucosinolates varies with the chemical nature of the glucosinolate side chain. For example, if 4-methylthiobutyl glucosinolate is oxidized, it generates the anticarcinogenic 4-methylsulfinylbutyl glucosinolate (Figure 1). However, if this product undergoes two additional reactions to generate the 2-hydroxy-3-butenyl glucosinolate, the product is goitrogenic without significant anticancer activity (Faulkner et al., 1998). Thus, it will be advantageous to manipulate glucosinolate structures to alter the nutritional and economic value of a food crop. This variation in glucosinolate structure and corresponding activity provides a useful system in which to investigate both the evolutionary and biological aspects of secondary metabolism.

In this article, we report the molecular basis of the natural variations for the presence of the *GS-ALK* (alkenyl producing) and *GS-OHP* (hydroxyalkyl producing) reactions in Arabidopsis (Figure 1). We have identified a single region that controls both reactions. In this region, there was a small gene family of 2-oxoglutarate–dependent dioxygenases that result from a gene duplication that apparently led to the evolution of two different enzymatic reactions. We present data showing that one member of this gene family controls the *GS-ALK* reaction and a second member controls the *GS-OHP* reaction. Importantly, natural variations at these genes predict glucosinolate concentration and type in Arabidopsis ecotypes.

RESULTS

Cosegregation of *GS-ALK*, *GS-OHP*, and *GS-AOP^{null}*

Previous reports found variations within Arabidopsis and within the genera *Thlaspi* and *Malcolmia*, also in the family Brassicaceae, for the presence of alkenyl, methylsulfinylalkyl, and hydroxyalkyl glucosinolates (Figure 1). These differences have been ascribed to the *GS-ALK* and *GS-OHP* loci (Giamoustaris and Mithen, 1996), which are alleles of the same locus or tightly linked loci. Both the *GS-ALK* and *GS-OHP* variants map to the top of chromosome IV; thus, we re-

fer to them jointly as *GS-AOP* (Mithen et al., 1995). To map the *GS-AOP* region, we used 300 lines of the Landsberg *erecta* (L*er*) × Columbia (Col) recombinant inbred lines (RILs) and 162 lines of the L*er* × Cape Verde Islands (Cvi) RILs (Lister and Dean, 1993; Alonso-Blanco et al., 1998b). L*er* contains the *GS-OHP* product 3-hydroxypropyl glucosinolate as the predominant short-chain aliphatic glucosinolate, and Cvi contains the *GS-ALK* products allyl glucosinolate and 3-butenyl glucosinolate (Figure 2). The Col ecotype accumulates the 4-methylsulfinylbutyl glucosinolate, which is the presumed substrate of the enzyme activities represented by *GS-OHP* and *GS-ALK*, suggesting that this ecotype is null for both *GS-OHP* and *GS-ALK* (*GS-AOP^{null}*; Figure 2). In addition to the variations at GS-AOP, L*er*, Col,
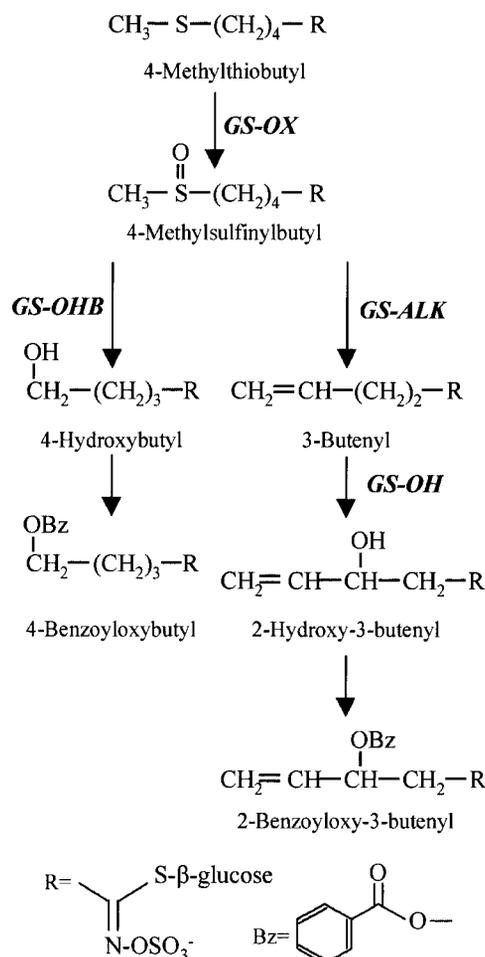
Figure 1. Side Chain Modifications of Methionine-Derived Glucosinolates in Arabidopsis.

Potential side chain modifications for the elongated methionine derivative C_4 dihomomethionine are shown. Steps with natural variation in Arabidopsis are shown in boldface to the right or left of each enzymatic arrow with the name of the corresponding locus.

and Cvi have variations at the previously described GS-Elong locus (J. Kroymann and T. Mitchell-Olds, unpublished data). Variation at GS-Elong leads to the production of aliphatic glucosinolates with either a three-carbon-atom (L*er*) or a four-carbon-atom (Cvi and Col) side chain.

Of the 300 L*er* × Col RILs, 152 lines produced principally C_3 glucosinolates, with 79 accumulating 3-hydroxypropyl glucosinolate, indicative of *GS-OHP*, and 73 containing the *GS-AOP^{null}* 3-methylsulfinylpropyl glucosinolate. All of the 148 L*er* × Col RILs with predominantly C_4 glucosinolates accumulated 4-methylsulfinylbutyl glucosinolate, with no lines containing 4-hydroxybutyl glucosinolate instead of the 1:1 mix of 4-methylsulfinylbutyl to 4-hydroxybutyl glucosinolate, as expected. This finding suggests that the enzyme encoded by the *GS-OHP* locus is unable to catalyze the conversion of 4-methylsulfinylbutyl glucosinolate to 4-hydroxybutyl glucosinolate and has specificity for substrates with side chains of three carbon atoms (Giamoustaris and Mithen, 1996). This further supports the theory that methylsulfinylalkyl accumulation is indicative of a nonfunctional *GS-AOP* variant. In addition to containing mostly C_4 glucosinolates, many of these 148 RILs also contained minor levels of C_3 glucosinolates, making it possible to score *GS-OHP*. Analysis of C_3 glucosinolates showed that 65 lines contained 3-methylsulfinylalkyl and 58 lines accumulated 3-hydroxypropyl. The other 25 lines contained no detectable C_3 glucosinolates; therefore, we were unable to score them for *GS-OHP*. In total, 138 of the L*er* × Col RILs scored as *GS-AOP^{null}* and 137 scored as *GS-OHP*. This 1:1 segregation further supports the theory that *GS-OHP* and *GS-AOP^{null}* are two alleles of the same gene or are in close proximity in the genome.

To test the linkage of the *GS-ALK* and *GS-OHP* variants in Arabidopsis, we analyzed the 162 L*er* × Cvi RILs. Like L*er* × Col, this population segregated for different alleles of *GS-AOP* and GS-Elong. In lines that generated C_3 glucosinolates, 42 produced 3-hydroxypropyl glucosinolate and 24 produced allyl glucosinolate. In the C_4 glucosinolate–producing lines, 72 produced butenyl and allyl glucosinolates, and 28 produced primarily 4-methylsulfinylbutyl glucosinolate, with minor amounts of 3-hydroxypropyl glucosinolate. This finding is in agreement with the previous observation that *GS-OHP* is C_3 specific and unable to convert the 4-methylsulfinylbutyl to 4-hydroxybutyl glucosinolate. In contrast, *GS-ALK* was able to convert at least the C_3 and C_4 methylsulfinylalkyl glucosinolates to alkenyl glucosinolates. In total, 96 of the L*er* × Cvi RILs scored as *GS-ALK* and 70 lines scored as *GS-OHP*. This nearly 1:1 segregation pattern and the lack of recombinant individuals containing both the *GS-OHP* and *GS-ALK* phenotypes suggest that they are alleles of the same locus or map within close proximity. Furthermore, the *GS-AOP* region in the L*er* × Cvi recombinant inbred population had a significant effect on the accumulation of aliphatic glucosinolates such that the *GS-ALK* lines had threefold higher glucosinolate levels than did the *GS-OHP* lines (P < 0.00001; R^2 = 0.31). This suggests that *GS-AOP* is a major determinant of glucosinolate concentration in

these lines. Together, the two populations of RILs suggest that the methylsulfinyl, hydroxyl, and alkenyl *GS-AOP* variants are alleles of the same locus or within a small genetic region in Arabidopsis, because there was no recombination between the variants in 462 lines. Furthermore, we were unable to identify any recombinant progeny in 5000 F2 progeny from a L*er* × Col cross. If these variants represent alleles at two different loci, they are very tightly linked.
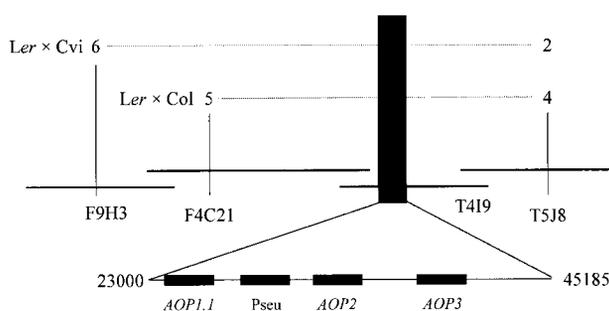
Fine-Scale Mapping of *GS-AOP*

Comparison of markers mapped previously in the L*er* × Col recombinant inbred population with the *GS-AOP* phenotype placed *GS-ALK* and *GS-AOP^{null}* at the top of chromosome IV, as described previously (Mithen et al., 1995). As shown
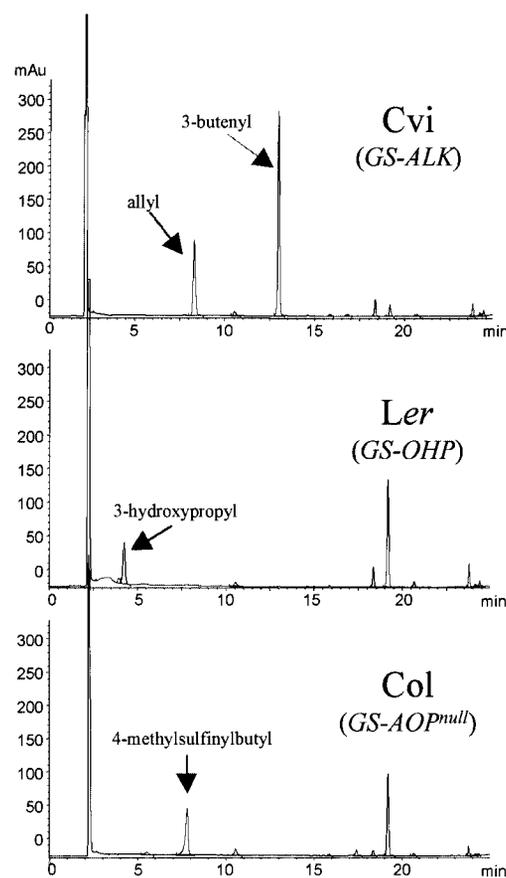
Figure 2. HPLC Results of L*er*, Cvi, and Col Glucosinolate Profiles.

Shown are HPLC results monitored at 229 nm of samples from L*er*, Cvi, and Col prepared from equal amounts of 2-week-old rosette tissue. The major methionine-derived glucosinolate peaks are labeled for each ecotype. The large peak at ∼18.5 min in L*er* and Col is a tryptophan-derived glucosinolate. The large peak at ∼2.5 min is due to solvent mixing from the injected sample. mAu, milliabsorbance units.

Figure 3. Fine-Scale Map of *GS-AOP*.

A fine-scale genomic map of *GS-AOP* is shown for reference. Horizontal solid lines represent the four BACs used, and the vertical lines represent the positions of the microsatellites on each BAC. The number to the right of each recombinant inbred population name is the number of recombinations between the given marker and the *GS-AOP* phenotype. The vertical black bar represents the genomic location of the three 2-ODD genes. The three 2-ODD genes and one related 2-ODD pseudogene are labeled *AOP1*, *AOP2*, *AOP3,* and Pseu, respectively. The F9H3 and T5J8 microsatellite markers are separated by ∼300 kb. The dotted line indicates the region between the two microsatellite markers for the L*er* × Cvi cross (top line) or the L*er* × Col cross (bottom line).

in Figure 3, we fine-scale mapped *GS-AOP* to the region between microsatellite markers T5J8 and F4C21. This placed *GS-AOP* on three possible bacterial artificial chromosomes (BACs): F4C21, T4I9, and T5J8. Analysis of the L*er* × Cvi RILs amplified fragment length polymorphism (AFLP) map also placed *GS-ALK* and *GS-OHP* at the top of chromosome IV (5-centimorgan centromeric from GS.250C and 17-centimorgan telomeric of CH.169.C; Alonso-Blanco et al., 1998b). Fine-scale mapping in this cross placed *GS-AOP* on the same BACs as those identified in the L*er* × Col cross (Figure 3). In this region, the Col sequence from BAC T4I9 contains a small family of candidate genes. We identified three putative functional and one pseudo 2-oxoglutarate–dependent dioxygenase (2-ODD) genes (Figure 3). 2-ODDs are non-heme-iron–containing dioxygenases that typically use molecular oxygen, 2-oxoglutarate, ascorbate, and ferrous ions to catalyze substrate hydroxylations and other oxidations (Prescott, 1993). The reactions catalyzed by the *GS-OHP* and *GS-ALK* gene products, the conversion of methylsulfinylalkyl glucosinolates to alkenyl or hydroxypropyl glucosinolates, could plausibly be catalyzed by 2-ODDS. We have named these genes *AOP1*, *AOP2*, and *AOP3* (Figure 3). The three AOP genes appear to result from a gene duplication event, because a BlastN search on GenBank produced no other homologs of significant similarity. Amino acid comparison showed that the three genes are ∼60 to 70% similar to each other and ∼25% similar to other 2-ODD genes (data not shown). The pseudogene is a partial open reading frame that contains several frameshift mutations. The presence of a small gene family in a restricted region

could explain why two different enzymatic activities map to the same region.

Differential Expression of *AOP2* and *AOP3* Is Correlated with *GS-ALK* and *GS-OHP*

To investigate the association of the AOP genes with the already documented variation in glucosinolate phenotype, we developed primers that specifically recognize the corresponding full-length cDNAs for each gene. These primers first were tested on genomic DNA from L*er*, Col, and Cvi and shown by gel analysis and sequencing to amplify the expected fragment from each ecotype (data not shown). This demonstrates that the primers will recognize the corresponding cDNA from each ecotype. We then used these primers for quantitative reverse transcription–polymerase chain reaction (RT-PCR) detection of the different cDNAs. As shown in Figure 4, the *AOP1* and *Ran* (control) genes are expressed at similar levels in all three ecotypes. However, we detected *AOP3* cDNA only in the *GS-OHP*–containing L*er* and not in the *GS-ALK*–containing Cvi or *GS-AOP*[null]–containing Col (Figure 4). This finding suggests that *AOP3* may be responsible for the *GS-OHP* reaction. In contrast with *AOP3*, *AOP2* expression was detected only in the *GS-ALK* Cvi ecotype and the *GS-AOP*[null] Col ecotype, with Cvi containing higher levels than Col (Figure 4). Sequencing of the *AOP2* cDNA from Cvi and Col showed that the Cvi sequence contains a full-length 2-ODD, whereas the Col cDNA contains a 5-bp deletion that leads to a nonfunctional protein (data not shown). Thus, functional *AOP2* is present only in the *GS-ALK*–containing ecotype. Furthermore, this
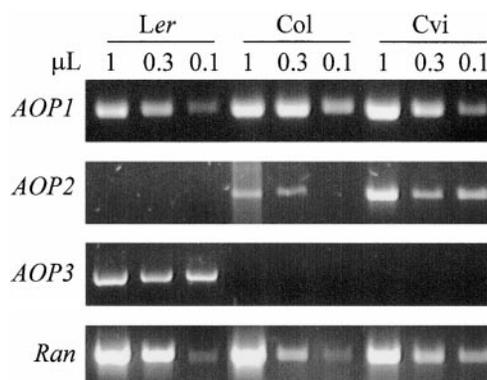
Figure 4. Ecotype-Specific Expression of the AOP Genes.

Shown are the ethidium bromide–stained gels from a quantitative RT-PCR experiment with the L*er*, Col, and Cvi parental ecotypes. The *Ran* gene was used as a loading control. Numbers above the gels (1, 0.3, and 0.1) indicate the amounts of cDNA (μL) used for the RT-PCRs.

Table 1. Genetic Association of GS-AOP Phenotype with AOP Expression[a]

| Ecotype | GS-AOP | AOP2 | | AOP3 Exp | AOP1.1 Exp | AOP1.2 Exp |
		Exp[b]	Fxnl[c]			
Cal-0	ALK	+	+	−	+	−
Cnt-1	ALK	+	+	−	+	−
Kondara	ALK	+	+	−	+	−
Cvi	ALK	+	+	−	+	−
Ema-1	ALK	+	+	−	+	−
Hodja	ALK	+	+	−	+	−
Kas-1	ALK	+	+	−	+	−
Mrk-0	ALK	+	+	−	+	−
Sorbo	ALK	+	+	−	+	−
Su-0	ALK	+	+	−	+	−
Tac	ALK	+	+	−	+	−
Yo-0	ALK	+	+	−	+	−
Per-1	Null	+	−	−	+	−
Col	Null	+	−	−	+	−
Bl-1	OHP	−		+	−	+
Ka-0	OHP	−		+	−	+
L*er*	OHP	−		+	−	+
Lip-0	OHP	−		+	−	+
Pet	OHP	−		+	−	+
Pi-0	OHP	−		+	−	+
Wei-0	OHP	−		+	−	+

[a] (+), the presence of mRNA expression and/or functional protein; (−), the absence of mRNA expression or nonfunctional protein.
[b] Exp, expression.
[c] The sequence contains no premature stop codons or frameshift mutations.

agrees with the observation that the *GS-AOP^null* allele in Col is a null allele of both *GS-ALK* and *GS-OHP*, because Col does not express *AOP3* or contain functional *AOP2*.

Ecotype Association Study

To further test the relation between the AOP genes and natural variations in glucosinolate biosynthesis, we analyzed 21 Arabidopsis ecotypes for AOP gene expression and glucosinolate phenotype. As shown in Table 1, this analysis revealed a complete association between glucosinolate profiles and AOP gene expression. All ecotypes that expressed functional *AOP2* accumulated the alkenyl glucosinolate and did not express *AOP3* (Table 1). These observations support the hypothesis that *AOP2* is responsible for *GS-ALK*. The hypothesis that *AOP3* is responsible for the hydroxylation reaction is supported by the observation that *AOP3* is expressed only in those ecotypes that produce the hydroxyalkyl glucosinolates (Table 1). Thus, expression of functional *AOP3* is completely associated with the *GS-OHP* variant, and expression of functional *AOP2* is completely associated with *GS-ALK*. Furthermore, both ecotypes that accumulate methylsulfinylalkyl glucosinolate, Col and Per-1, do not ex-

press *AOP3* and contain the *AOP2* copy that has a 5-bp frameshift mutation that destroys its function (Table 1). Therefore, the absence of *AOP2* and *AOP3* leads to the accumulation of the methylsulfinylalkyl precursor.

Biosynthetic Capacity of Heterologously Expressed *AOP2* and *AOP3*

To test the hypothesis that *AOP2* is responsible for the *GS-ALK* reaction and *AOP3* is responsible for the *GS-OHP* reaction, we heterologously expressed thioredoxin fusion proteins for AOP2 and AOP3 in Escherichia. Each gene was cloned into the vector as a full-length cDNA by using the native stop codon, and the corresponding fusion protein was expressed in an arabinose-dependent manner. Crude extracts from induced and uninduced bacterial cultures were incubated with 3-methylsulfinylpropyl glucosinolate and 4-methylsulfinylbutyl glucosinolate to test the activity of the induced fusion proteins. As shown in Figure 5, induced AOP2 bacterial extracts catalyzed the conversion of the 3-methylsulfinylpropyl to the allyl glucosinolate and the 4-methylsulfinylbutyl to the 3-butenyl glucosinolate (cf. Figures 5A with 5B and 5C with 5D). The identities of the allyl and 3-butenyl
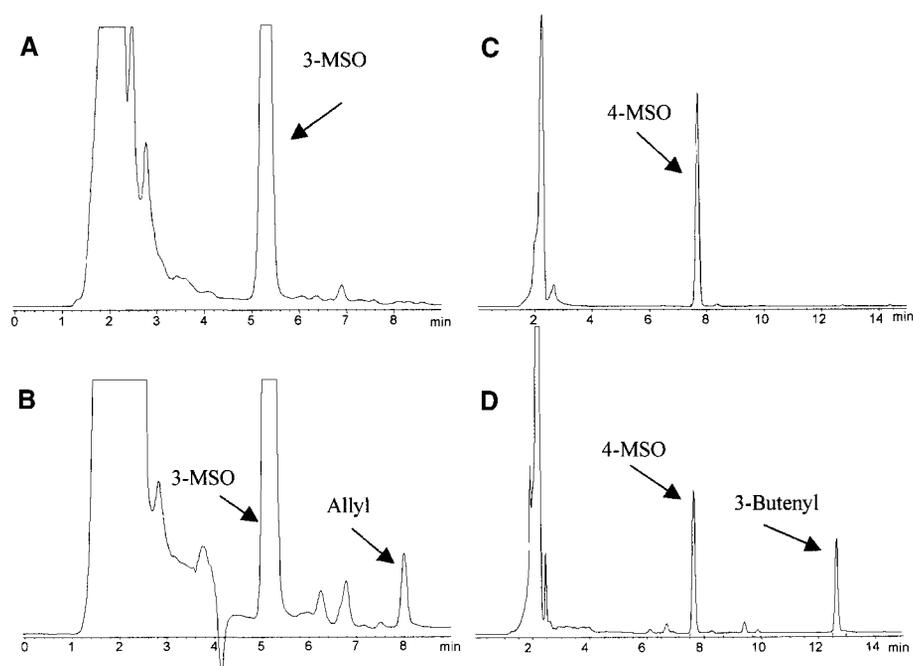
Figure 5. Enzymatic Activity of Heterologously Expressed *AOP2*.

HPLC results (monitored at 229 nm) of purified desulfoglucosinolates from bacterial extracts containing heterologously expressed *AOP2* fusion proteins are shown. All compound identities were confirmed by comparison of both retention times and UV light absorption profiles with those of authentic standards. 3-MSO, 3-methylsulfinylalkyl glucosinolate; 4-MSO, 4-methylsulfinylalkyl glucosinolate.

(A) Extract from 3-methylsulfinylalkyl glucosinolate treated with uninduced *AOP2* bacterial extract.

(B) Extract from 3-methylsulfinylalkyl glucosinolate treated with *AOP2* enzyme.

(C) Extract from 4-methylsulfinylalkyl glucosinolate treated with uninduced *AOP2* bacterial extract.

(D) Extract from 4-methylsulfinylalkyl glucosinolate treated with *AOP2* enzyme.

products were confirmed by coincidence of retention time and UV light spectra with those of authentic standards and by liquid chromatography–mass spectrometry. The uninduced bacterial extract produced neither of these products (data not shown). The two peaks at 6.2 and 6.8 min are bacterial contaminants that copurified with the glucosinolates. This finding shows that AOP2 is capable of catalyzing the *GS-ALK* reaction with both the 3-methylsulfinylalkyl and 4-methylsulfinylalkyl glucosinolates.

In contrast with AOP2, the induced bacterial extracts with the AOP3 constructs displayed a weak conversion of 3-methylsulfinylpropyl glucosinolate to 3-hydroxypropyl glucosinolate, as determined by retention time and diode array spectral comparisons with purified 3-hydroxypropyl glucosinolate (Figure 6). Insufficient material was available to confirm the identity of 3-hydroxypropyl glucosinolate by liquid chromatography–mass spectrometry. We were unable to show any conversion of 4-methylsulfinylbutyl glucosinolate to 4-hydroxybutyl glucosinolate (data not shown). Analysis of the bacterial extracts by SDS-PAGE showed that the

AOP3 fusion protein was insoluble, which could explain the very low activity of AOP3. These data support the idea that the natural variation in Arabidopsis for the production of hydroxyl and alkenyl glucosinolates can be explained by *AOP2* encoding the *GS-ALK* enzyme and *AOP3* controlling the *GS-OHP* reaction.

Analysis of AOP Genes

To analyze the effect of gene duplication and independent evolution on secondary metabolism, we sequenced the *AOP1*, *AOP2*, and *AOP3* genes from the L*er*, Cvi, and Col ecotypes. The cDNA primers were used to amplify both genomic DNA and cDNA from all three ecotypes. The *AOP2* cDNA from the *GS-ALK*–containing Cvi is 1296 nucleotides in length and encodes a protein of 432 amino acids. As mentioned above, the cDNA and genomic DNA for *AOP2* in the *GS-AOP^null*–containing Col contains a 5-bp deletion at base 484, which generates a frameshift mutation and results in a

severely truncated protein. Interestingly, the *AOP2* cDNA sequence obtained from L*er* genomic DNA shows that the open reading frame is intact and that the sequence is similar to that of Cvi (Figure 7). This finding suggests that the functional difference in phenotype between L*er* and Cvi is due to an expression polymorphism and that if *AOP2* were expressed in L*er* it would accumulate alkenyl glucosinolates (Figure 4).

We next analyzed variation in *AOP3*. The *AOP3* cDNA from the hydroxyalkyl glucosinolate–forming L*er* is 1230 nucleotides in length and encodes a 410–amino acid protein. *AOP3* cDNA sequences obtained from both Col and Cvi genomic sequences show that these genes are highly related to the L*er AOP3* sequence. *AOP1* cDNA has a sequence of 960 to 966 nucleotides that predicts a protein of 320 to 322 amino acids. The difference in length is due to variation in a GAT trinucleotide microsatellite within the *AOP1* open reading frame. In addition, we obtained two different sequences from the L*er AOP1* genomic DNA. One sequence corresponded to the expressed *AOP1* cDNA, whereas the other sequence was more closely related to *AOP1* from Cvi and Col (Figure 7). This finding suggests that L*er* contains a duplication of *AOP1* and that the original *AOP1* has somehow been silenced. We have named the original *AOP1* gene *AOP1.1* and the duplicated L*er* copy *AOP1.2*. Mapping of

AOP1.2 showed that the gene was tightly linked to the AOP region, but we were unable to obtain a precise genomic location (data not shown).

Interestingly, analysis of *AOP1* showed that *AOP1.1* is expressed only in the *GS-ALK* and *GS-AOP^null* ecotypes and that *AOP1.2* is expressed only in *GS-OHP* lines (Table 1). The presence of functional *AOP1.1* in the methylsulfinylalkyl lines suggests that *AOP1* is not responsible for the formation of alkenyl glucosinolates. Furthermore, heterologously expressed AOP1.1 or AOP1.2 did not convert purified methylsulfinylalkyl or methylthioalkyl to either alkenyl or hydroxyalkyl glucosinolates (data not shown). In addition, the AOP1.1/AOP1.2 duplication is younger than the speciation event between *Arabidopsis thaliana* and *A. lyrata* (Figure 7). Thus, this duplication is much too young to explain the presence of *GS-ALK/GS-OHP* variation in Arabidopsis and the genera *Thlaspi* and *Malcolmia*, also in the family Brassicaceae (Daxenbichler et al., 1991). Consequently, AOP1 probably plays no role in *GS-AOP* variation. However, it is possible that *AOP1* plays another role in the production of aliphatic glucosinolates. Additional work is required to determine if *AOP1* has a role in aliphatic glucosinolate biosynthesis or if the relation with *GS-AOP* variation is due to evolutionary history.
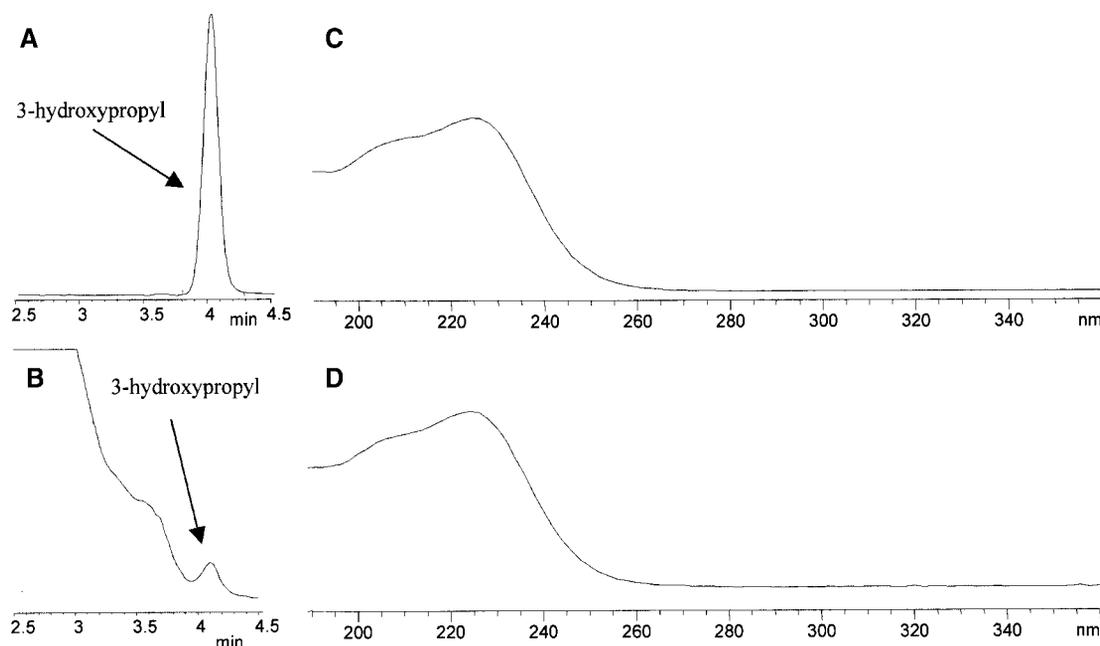
**Figure 6.** Enzymatic Activity of *AOP3* Heterologously Expressed in *Escherichia coli*.

E. coli extract was assayed with 3-methylsulfinylpropyl glucosinolate, and products were extracted and analyzed by HPLC as described in Methods.
(A) Sample of authentic 3-hydroxypropyl glucosinolate (monitored at 229 nm).
(B) Extract from *AOP3* enzyme assay with 3-methylsulfinylpropyl glucosinolate as substrate (monitored at 229 nm).
(C) Diode array spectrum of standard 3-hydroxypropyl desulfoglucosinolate in **(A)**.
(D) Diode array spectrum of 3-hydroxypropyl desulfoglucosinolate produced by *AOP3* in **(B)**.
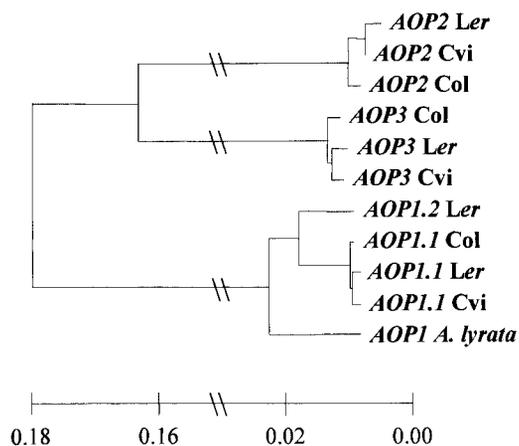
Figure 7. Tree of AOP cDNAs from L*er*, Cvi, and Col.

Cladogram of the relations of *AOP1*, *AOP2*, and *AOP3* from the L*er*, Cvi, and Col reference ecotypes. Either experimental cDNA sequences or predicted cDNA sequences from genomic sequences were used for the alignments shown. The scale was reduced between 0.02 and 0.16, and midpoint branching was used for this tree. Each sequence is listed with the ecotype from which it was obtained. *AOP1 A. lyrata* was obtained from *A. lyrata*.

DISCUSSION

AOP2 and *AOP3* Control the Formation of Alkenyl and Hydroxyalkyl Glucosinolates

Arabidopsis contains natural variation for the production of methylsulfinylalkyl, hydroxyalkyl, and alkenyl glucosinolates. The locus controlling this variation mapped to the top of chromosome IV near a small gene family of 2-ODD genes, which could catalyze the conversion of methylsulfinylalkyl glucosinolate to hydroxyalkyl or alkenyl glucosinolate. Enzyme assays of heterologously expressed fusion protein showed that the *AOP2* enzyme catalyzes the conversion of methylsulfinylalkyl glucosinolates to alkenyl glucosinolates and that the *AOP3* enzyme catalyzes the formation of hydroxyalkyl glucosinolates (Figures 5 and 6). Analysis of the 2-ODD cDNAs from 21 ecotypes showed that expression of functional *AOP2* is perfectly correlated with the products of the *GS-ALK* reaction and that expression of *AOP3* is completely associated with the products of the *GS-OHP* reaction. This finding was supported further by the presence of a frameshift mutation in the Col and Per-1 *AOP2* genes, which evidently caused a *GS-AOP^{null}* mutant and accumulation of the *GS-AOP* precursor, methylsulfinylalkyl glucosinolate. Thus, these experiments show that *AOP2* is responsible for the *GS-ALK* reaction and that *AOP3* is responsible for the *GS-OHP* reaction (Figure 8). In addition, the absence of ei-
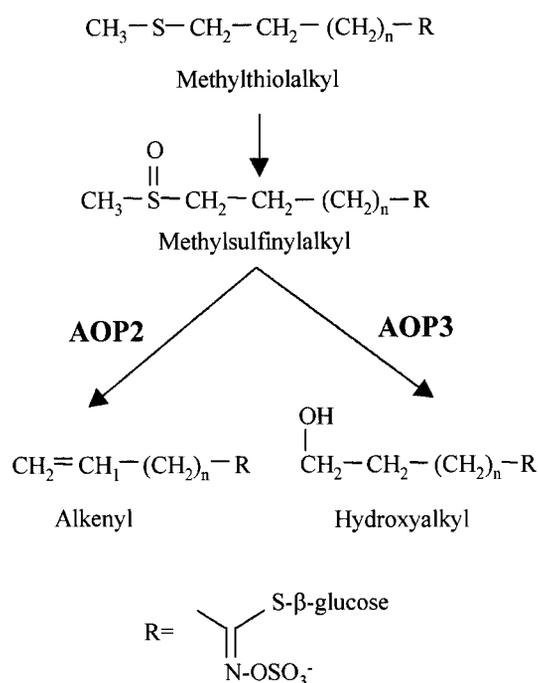
ther enzyme leads to the accumulation of the precursor methylsulfinylalkyl glucosinolate.

Role of Gene Duplication in the Evolution of *AOP2* and *AOP3*

BlastN searches with *AOP1*, *AOP2*, and *AOP3* showed that they are their own closest homologs and that they appear to be the result of two different gene duplication events. The first event separated *AOP1* from the *AOP2/3* progenitor, and the second event led to the formation of *AOP2* and *AOP3*. After the gene duplications, the separate copies were able to evolve new enzymatic functions. In this case, *AOP2* evolved the *GS-ALK* function, *AOP3* evolved the *GS-OHP* function, and *AOP1* appears to have a third, unidentified function. The length of the branches linking *AOP2* and *AOP3* suggests that the duplication occurred long before the separation of *A. lyrata* from *A. thaliana* (Figure 7). This finding agrees with previous data showing that *GS-ALK/GS-OHP* variation occurs in the distantly related Arabidopsis and in the genera *Thlaspi* and *Malcolmia* (Daxenbichler et al., 1991). The identification of this gene duplication that apparently led to two different enzymatic reactions using the same precursor will allow us to study the biochemical and structural mechanisms leading to these different reactions. It will be interesting as well to identify the reaction catalyzed by *AOP1*, which should increase our understanding of the evolutionary change involved in generating the new product/substrate specificities present in *AOP2* and *AOP3*.

Role of Amino Acid Evolution versus Promoter Mutation in the Evolution of *GS-AOP*

An unresolved question in evolutionary genetics concerns the importance of amino acid substitution versus promoter mutation in generating natural phenotypic variations. We found that the natural variation for the *GS-ALK* and *GS-OHP* reactions is due primarily to changes in the expression of the *AOP2* and *AOP3* genes (Figure 4). In the *GS-ALK* ecotypes, *AOP2* is expressed but *AOP3* is apparently silent. Conversely, in the *GS-OHP* ecotypes, *AOP3* is expressed and *AOP2* is silent (Table 2). Because the genomes of all ecotypes tested contain the genes for both *AOP2* and *AOP3* (data not shown), the major mechanism leading to the natural variation between *GS-ALK* and *GS-OHP* is promoter changes in the corresponding genes. Hence, analysis of the *AOP2* and *AOP3* promoter sequences in the different ecotypes will help elucidate the mechanisms that control the expression of these glucosinolate biosynthetic genes. In contrast with the *GS-ALK* versus *GS-OHP* variation, the observed variation between *GS-AOP^{null}* and *GS-ALK/GS-OHP* is the result of a 5-bp deletion that generates a truncated *AOP2* open reading frame and presumably generates an in-

$$CH_3-S-CH_2-CH_2-(CH_2)_n-R$$

Methylthiolalkyl

$$CH_3-\overset{\overset{\displaystyle O}{\|}}{S}-CH_2-CH_2-(CH_2)_n-R$$

Methylsulfinylalkyl

AOP2   **AOP3**

$$CH_2=CH_1-(CH_2)_n-R \qquad \overset{\overset{\displaystyle OH}{|}}{CH_2}-CH_2-(CH_2)_n-R$$

Alkenyl   Hydroxyalkyl

$$R=\ \overset{\displaystyle S\text{-}\beta\text{-glucose}}{\underset{\displaystyle N\text{-}OSO_3^-}{\diagup}}$$

Figure 8. Putative Enzymatic Reactions for the 2-ODD Genes in the GS-AOP Region.

The molecular structures and putative enzymatic reactions catalyzed by the AOP2 and AOP3 enzymes are shown. Side chains of up to eight carbon atoms ($n = 6$) are known in Arabidopsis. Heterologous expression studies demonstrated the conversion of methylsulfinylalkyl glucosinolates to their alkenyl and hydroxyalkyl derivatives for three-carbon-atom side chains (propyl; $n = 1$). For glucosinolates with four-carbon-atom side chains (butyl; $n = 2$), only the methylsulfinylalkyl-to-alkenyl conversion was demonstrated.

active protein. Therefore, the natural variation between *GS-ALK* and *GS-AOP^{null}* is due to the functionality of the protein. Thus, both variation in promoters and protein function have strong effects on phenotypic variation in Arabidopsis glucosinolates.

GS-AOP Variation and Speciation

Published reports have shown that other Brassicaceae species contain variation for *GS-ALK* versus *GS-OHP*. For example, species within the genera *Thlaspi* and *Malcolmia*, both within the Brassicaceae, vary for the presence of the two reactions (Daxenbichler et al., 1991). Thus, the variation for the two different classes of glucosinolate is found in species that diverged more than 10 million years ago (Koch et al., 1999). One possible explanation for this wide variation in the *GS-ALK* and *GS-OHP* reactions is that *AOP2* and *AOP3* arose before these species diverged. The presence of one

gene or the other within a given species may lead to the natural variation. This presents the possibility that the presence of an environmental pressure, such as heterogeneous selection, maintains the variation. The role of *AOP2/3* in controlling this variation in other species will be tested by correlating the presence of *AOP2* or *AOP3* with the *GS-ALK* or *GS-OHP* reactions in numerous species.

GS-AOP Variation Controls the Level of Leaf Aliphatic Glucosinolates

Analysis of the L*er* × Cvi recombinant inbred line studies showed that the *GS-ALK* variant increased leaf aliphatic glucosinolates up to threefold over either the *GS-OHP* or the *GS-AOP^{null}* variant (P < 0.00001; $R_2 = 30.1$). This shows that *GS-AOP* has a significant level of control over the total aliphatic glucosinolate concentration in the leaf. One possible explanation for this is that glucosinolate biosynthesis is regulated via a feedback mechanism in which the alkenyl glucosinolate is not sensed as well as the hydroxyalkyl or methylsulfinylalkyl glucosinolate is sensed. Thus, it may be possible to change glucosinolate concentrations in vegetables and forage crops merely by altering side chain modification. Future quantitative trait loci mapping studies will enable us to discover the mechanisms that control these differences.

Seed versus Leaf AOP Phenotype

Our data suggest that *AOP2* and *AOP3* control the decision between producing alkenyl and hydroxypropyl glucosinolates in the leaves of Arabidopsis. However, as has been described previously, the seeds of Col-0 contain 4-hydroxybutyl and 4-methylsulfinylbutyl glucosinolate (Hogge et al., 1988). Analysis of segregation in the L*er* × Col-0 RILs suggests that the production of 4-hydroxybutyl glucosinolate in the seed is regulated by a locus other than *GS-AOP* (D.J. Kliebenstein and T. Mitchell-Olds, unpublished data). This locus could possibly encode one of the numerous other 2-ODDs present in the Arabidopsis genome. This second locus suggests that there may be multiple loci controlling similar side chain modifications in Arabidopsis. However, this does not diminish the observation that *GS-AOP* as a major determinant of glucosinolate side chain structure in Arabidopsis.

Future

The identification of these genes from Arabidopsis provides an opportunity to modify the composition of glucosinolate side chains in other species. For example, identification of the homologous genes in some brassicaceous food crops

Table 2. AOP Primers

Name	Repeat	Sequence	L*er*	Col	Cvi
F9H3-F	TA	TTGCCAAAATTTCTGTAGCA	126	130	122
F9H3-R		CTCGACGACTTGTTGTTGGT			
T5J8-F1	GAA	GCCAAGACGCAGAAGAAGAG	125	150	225
T5J8-R1		TCTCATTATTCCCCACAATGC			
F4C21-F	TA	GCGCTTCATCTAGTTACGCTTT	165	171	167
F4C21-R		CCCGGACTGAACCAAACTAA			
T5J8-F2	TA	CGATCATCGGTGTTCACCTT	160	125	140
T5J8-R2		GAAAATAAATCGTCATATGGTGTACTG			
AOP1-F		ATGGATTCAGACTTTGTTCCT			
AOP1-R		AAAGGCAGCGAAAGCATGG			
AOP2-F		ATGGGTTCATGCAGTCTTCA			
AOP2-R		TGCTTCGGAGACGGCACAAT			
AOP3-F		ATGGGTTCATGCAGTCCTC			
AOP3-R		TTTCCCAGCAGAGACGCC			

could allow modification of the nutritional aspects of these crops. Analysis of the evolution of the different enzymatic activities of AOP2 and AOP3 also will suggest a means to study the generation of novel enzymatic activities involved in secondary metabolism through gene duplication.

METHODS

Ninety-Six–Well Glucosinolate Extraction and Purification

The glucosinolate extraction and purification technique follows the basic sephadex/sulfatase Arabidopsis protocol previously described (Hogge et al., 1988). Samples were harvested into deep-well microtiter tubes (either 10 fresh leaf discs frozen in liquid nitrogen, 10 mg of freeze-dried leaf material, or 5 mg of dried seeds). Four 2.3-mm ball bearings were added, and the samples were ground into a fine powder in a paint shaker by high-speed agitation. To extract glucosinolates, we added 400 μL of methanol, 10 μL of 0.3 M lead acetate, and either 120 μL of water for seeds and freeze-dried material or 80 μL of water for fresh tissue. The samples were mixed for 1 min in the paint shaker and allowed to incubate for 60 min at 180 rpm on a rotary shaker. The tissue and protein were pelleted by centrifuging at 2500*g* for 10 min, and the supernatant was used for anion-exchange chromatography. Ninety-six–well filter plates from Millipore (model MAHVN4550) were loaded with 45 μL of DEAE Sephadex A-25 by using the Millipore multiscreen column loader. Then, 300 μL of water was added and allowed to equilibrate for 2 to 4 hr. After water was removed with 2 to 4 sec of vacuum on the Qiagen vacuum manifold, 150 μL of the supernatant was added to the 96-well columns, and the liquid was removed by 2 to 4 sec of vacuum. This step was repeated once to bring the total volume of plant extract to 300 μL. The columns were washed four times with 150 μL of 67% methanol, three times with 150 μL of water, and three times with 150 μL of 1 M sodium acetate. To desulfate glucosinolates on the column, we added 10 μL of water and 10 μL of sulfatase solution to each column, and the plates were incubated overnight at room temperature (Hogge et al., 1988). Desulfoglucosinolates were eluted by placing a deep-well 2-mL 96-well plate in the bottom of the 96-well vacuum

manifold and aligning the 96-well column plate. The DEAE Sephadex then was washed twice with 100 μL of 60% methanol and twice with 100 μL of water.

HPLC

Forty microliters of the glucosinolate extract was run on a Hewlett-Packard Lichrocart 250-4 RP18e 5-μm column on a Hewlett-Packard 1100 series HPLC. Compounds were detected at 229 nm and separated using either of the two following programs with aqueous acetonitrile. For seeds, the program was an 8-min gradient from 1.5 to 5.0% acetonitrile, a 2-min gradient from 5 to 7% acetonitrile, a 32-min gradient from 7 to 52% acetonitrile, a 2-min gradient from 52 to 92% acetonitrile, 5 min at 92% acetonitrile, a 3-min gradient from 92 to 1.5% acetonitrile, and a final 8 min at 1.5% acetonitrile. For leaf material, the program was a 6-min gradient from 1.5 to 5.0% acetonitrile, a 2-min gradient from 5 to 7% acetonitrile, a 7-min gradient from 7 to 25% acetonitrile, a 2-min gradient from 25 to 92% acetonitrile, 6 min at 92% acetonitrile, a 1-min gradient from 92 to 1.5% acetonitrile, and a final 5 min at 1.5% acetonitrile.

Experimental Design

Five plants from each of the 162 Landsberg *erecta* (L*er*) × Cape Verde Islands (Cvi) recombinant inbred lines (RILs) were planted in 4-inch pots with one L*er* and one Cvi parental control pot per flat of 36 pots. The planting order was randomized for each of three experiments. The plants were grown for 3 weeks after planting under an 11-hr-light/13-hr-dark photoperiod, at which time 10 1.0-cm^2 leaf discs were harvested for glucosinolate extraction. The plants were allowed to mature, and the seed from the five plants were pooled. This procedure was repeated for three independent replicates for each line and 15 replicates for each parent.

The L*er* × Columbia (Col) RILs were given 3 days of cold treatment in the dark and then allowed to grow in a 16-hr-light/8-hr-dark photoperiod for 3 weeks. At 3 weeks, they were harvested and lyophilized. Glucosinolates were extracted from each leaf and seed sample three times, and the results are reported as the arithmetic mean of each ecotype or line.

Ninety-Six–Well DNA Extraction

Plants were grown for 3 weeks under a 9-hr-light/15-hr-dark photoperiod. At 3 weeks of age, one large leaf was harvested into a deep-well microtiter tube from Integra Bioscience (Fernwald, Germany). This procedure was repeated for 95 other samples until a full plate of 96 samples was obtained. The samples were frozen in liquid nitrogen and lyophilized overnight. Four 2.3-mm ball bearings from VandP Scientific (San Diego, CA) were added, and the samples were ground into a fine powder in a paint shaker. Three hundred fifty microliters of extraction buffer (200 mM Tris-HCl, pH 7.5, 250 mM NaCl, 25 mM EDTA, and 0.5% SDS) was added to each tube and incubated at 65°C for 1 hr. The tubes were removed and allowed to cool for at least 10 min. One hundred microliters of 5 M potassium acetate, pH 7.5, was added, and the samples were centrifuged for 15 min at 2500g to precipitate the protein and insoluble material. Two hundred twenty microliters of the supernatant was transferred to a 96-well microtiter plate (wells were 2 mL deep) that contained 220 μL of ice-cold isopropanol. The DNA was precipitated by centrifugation at 1800g for 15 min. The supernatant was removed by tipping the plate upside down, and the pellets were washed with 200 μL of 75% ethanol and centrifuged for 5 min at 1800g. The supernatant again was removed by tipping the plate upside down, and the plate was left overnight to dry at room temperature. Four hundred microliters of 100 mM Tris-HCl, pH 8.0, was added, and the pellet was dissolved for 10 min at 65°C. Forty microliters then was divided into aliquots on two to four microtiter plates, depending on the desired number of reactions. If the DNA was to be used for multiplex microsatellite reactions, it was reprecipitated and resuspended in one-tenth the initial volume of 100 mM Tris-HCl, pH 8.0.

Microsatellites

Previously published microsatellite primer sequences were obtained from the Arabidopsis Information Resource (www.arabidopsis.org). All other microsatellites were identified by scanning bacterial artificial chromosome (BAC) sequences obtained from the Arabidopsis Information Resource with RepeatMasker-Repetitive Element Filter (http://www.genome.washington.edu/UWGC/analysistools/repeatmask.htm; A.F.A. Smit and P. Green, unpublished data). The primers listed in Table 2 were used for fine-scale mapping. Five microliters of the resuspended 96-well DNA extraction DNA was added to 20 μL of polymerase chain reaction (PCR) mixture (2.5 mM MgCl$_2$, 200 picomoles primers, and 0.5 units of Taq). These then were run with the following cycle program: 95°C for 3 min; 40 cycles of 95°C for 20 sec, 56°C for 20 sec, and 72°C for 1 sec; 72°C for 3 min; and 4°C final. The polymorphisms were scored on 4% agarose. Mapping was done using Mapmaker version 3 (Lander et al., 1987).

Quantitative Reverse Transcription–PCR and cDNA Sequencing

Total RNA was isolated from ∼100 mg of leaf tissue using the Trizol reagent. Approximately 1 μg of total RNA was used for cDNA synthesis, as described (Frohman et al., 1988). For quantitative reverse transcription (RT)–PCR, 0.1, 0.3, or 1 μL of the resulting total cDNA was added to 25-μL PCRs with the gene-specific primers listed in Table 2. The resulting product was visualized on a 1.5% agarose gel stained with ethidium bromide. For cDNA sequencing, 1 to 8 μL of

the resulting total cDNA then was added to 25-μL PCRs with the gene-specific primers listed in Table 2 to amplify the corresponding specific cDNA. The resulting product then was separated on a 1.5% agarose gel, the band was removed, and the cDNA was purified with Qiagen (Valencia, CA) gel purification columns. The resulting cDNA was sequenced with the primers listed in Table 2 by using Perkin-Elmer Big Dye terminator chemistry on a Perkin-Elmer 310 sequencer. The sequences then were analyzed with the DNAstar analysis package (DNAstar, Madison, WI). Trees were generated using TREECON for Windows version 1.3b with 100 reiterations (Van de Peer and De Wachter, 1994).

Generation of Thioredoxin Fusion Proteins and Enzyme Assays

The cDNA primers listed in Table 2 were used to amplify the full-length cDNAs from *AOP1.1*, *AOP1.2*, *AOP2*, and *AOP3*. These cDNAs were used with the pBAD/Thio-E Echo Cloning System from Invitrogen (Carlsbad, CA). This places the cDNAs in a fusion protein with thioredoxin under the control of an arabinose-induced promoter. After cloning, the inserted cDNA was sequenced to verify the junctions and to verify that there had been no mutations due to PCR. The proteins were induced as described by the manufacturer (Invitrogen). The bacteria were pelleted and resuspended in 1 M Tris-HCl, pH 7.5, and lysed by five repetitive freeze–thaw cycles. Four hundred microliters of the crude lysate was used in reactions with the purified intact glucosinolate, as described, with the addition of 200 mM sucrose and the use of 10 mM oxoglutarate and 10 mM ascorbate instead of 40 mM of each of these (Hedden, 1991). The reactions were allowed to proceed for 4 hr at 28°C, and the glucosinolates then were purified and analyzed by HPLC or HPLC–mass spectrometry. We attempted to solubilize and/or stabilize the AOP3 fusion protein with 20% sorbitol, 10% glycerol, Triton X-100 (0.01, 0.05, or 0.1%), and Tween 20 (0.01, 0.05, or 0.1%). These were attempted individually and in all possible combinations.

Preparation of Intact Glucosinolates

Extracts were made using methods adapted from previously published protocols (Thies, 1979; Zrybko et al., 1997). Lyophilized samples (1 g) were immersed in boiling deionized water (40 mL) containing 100 μL of 0.3 M Pb(OAc)$_2$, and 0.3 M Ba(OAc)$_2$ solution for 10 min. After 20 min of gentle shaking at room temperature, samples were centrifuged at 4000g for 10 min. The supernatant fraction (extract) was cleaned by modification of the procedure of Thies (1988). The extract was loaded onto a DEAE Sephadex A25 column (1 g dry weight). The column was rinsed with 5 mL of water followed by 2 × 5 mL of formic acid:isopropanol:water (3:2:5 [v/v/v]) and 4 × 5 mL of water. Glucosinolates were eluted with 25 mL of 0.5 M K$_2$SO$_4$/3% isopropanol dropped into 25 mL of ethanol. After centrifugation (4000g for 10 min), the supernatant was evaporated, and the residue was transferred with 4 × 3 mL of methanol into a centrifuge tube. It was stored for 15 min at −20°C and centrifuged (4000g for 10 min), and the supernatant was evaporated. The residue was transferred with 2 × 0.5 mL of water into autosampler vials.

Separation of intact glucosinolates was achieved on a Hewlett-Packard 1100 series system with autosampler, column oven, and diode array detector as described (Zrybko et al., 1997) with some modifications. The procedure used a C-18, fully endcapped, reverse-phase

column (LiChrospher RP-18; 250 × 4.6 mm i.d., 5-μm particle size; Chrompack, Raritan, NJ) operated at 1 mL/min and 25°C. Injection volume was 30 μL. Elution was accomplished with a gradient (solvent A, 0.075% triethylamine and 0.05% trifluoroacetic acid in water; solvent B, methylcyanide) of 1% solvent B (6-min hold) and 1 to 30% solvent B (24 min) followed by a cleaning cycle (30 to 95% solvent B in 1 min, 3-min hold, 95 to 1% solvent B in 1 min, 10-min hold). Eluting compounds were monitored at 229 nm and collected with a fraction collector. The fractions containing single intact glucosinolates were evaporated nearly to dryness and reconstituted with 2 × 0.5 mL of 1 M Tris-HCl, pH 7.5.

Mass Spectrometry

Analysis of glucosinolates was performed on a Quattro II (Micromass Ltd. Altrincham, Cheshire, UK) tandem quadrupole mass spectrometer equipped with an atmospheric pressure chemical ionization source. The corona pin was operated at 3.5 kV, and the sample cone was operated at 16 V. HPLC was performed as described previously. Vaporization was achieved with a nitrogen sheath gas (300 L/hr) and drying gas (150 L/hr) at 400°C. Mass spectra of 3-methylsulfinylpropyl, 4-methylsulfinylbutyl, allyl, 3-butenyl, and 3-hydroxypropyl glucosinolates from the enzymatic reactions were analyzed with the first quadrupole set to detect a single $M+H^+$ specific for the glucosinolate being tested.

Statistics

Statistical analysis was performed using Systat version 7 (SPSS Inc., Chicago, IL).

REFERENCES

Alonso-Blanco, C., Peeters, A.J.M., Koornneef, M., Lister, C., Dean, C., Vandenbosch, N., Pot, J., and Kuiper, M.T.R. (1998b). Development of an AFLP based linkage map of Ler, Col and Cvi *Arabidopsis thaliana* ecotypes and construction of a Ler/Cvi recombinant inbred line population. Plant J. **14,** 259–271.

Back, K., and Chappell, J. (1996). Identifying functional domains within terpene cyclases using a domain-swapping strategy. Proc. Natl. Acad. Sci. USA **93,** 6841–6845.

Daxenbichler, M.E., Spencer, G.F., Carlson, D.G., Rose, G.B., Brinkler, A.M., and Powell, R.G. (1991). Glucosinolate composition of seeds from 297 species of wild plants. Phytochemistry **30,** 2623–2638.

Du, L., Lykkesfeldt, J., Olsen, C., and Halkier, B. (1995). Involvement of cytochrome P450 in oxime production in glucosinolate biosynthesis as demonstrated by an in vitro microsomal enzyme system isolated from jasmonic acid-induced seedlings of *Sinapis alba* L. Proc. Natl. Acad. Sci. USA **92,** 12505–12509.

Faulkner, K., Mithen, R., and Williamson, G. (1998). Selective increase of the potential anticarcinogen 4-methylsulphinylbutyl glucosinolate in broccoli. Carcinogenesis **19,** 605–609.

Frohman, M.A., Dush, M.K., and Martin, G.R. (1988). Rapid production of full-length cDNAs from rare transcripts: Amplification using a single gene-specific oligonucleotide primer. Proc. Natl. Acad. Sci. USA **85,** 8998–9002.

Giamoustaris, A., and Mithen, R. (1995). The effect of modifying the glucosinolate content of leaves of oilseed rape (*Brassica napus* ssp *oleifera*) on its interaction with specialist and generalist pests. Ann. Appl. Biol. **126,** 347–363.

Giamoustaris, A., and Mithen, R. (1996). Genetics of aliphatic glucosinolates. IV. Side-chain modification in *Brassica oleracea*. Theor. Appl. Genet. **93,** 1006–1010.

Halkier, B.A., and Du, L. (1997). The biosynthesis of glucosinolates. Trends Plant Sci. **2,** 425–431.

Hedden, P. (1991). Gibberellin biosynthetic enzymes and the regulation of gibberellin concentration. In Gibberellins; 1989 July 20–23; Tokyo, Japan, N. Takahashi, B.O. Phinney, and J. MacMillan, eds (New York: Springer-Verlag).

Hogge, L.R., Reed, D.W., Underhill, E.W., and Haughn, G.W. (1988). HPLC separation of glucosinolates from leaves and seeds of *Arabidopsis thaliana* and their identification using thermospray liquid chromatography-mass spectrometry. J. Chromatogr. Sci. **26,** 551–556.

Koch, M., Bishop, J., and Mitchell-Olds, T. (1999). Molecular systematics of *Arabidopsis* and *Arabis*. Plant Biol. **1,** 529–537.

Lander, E.S., Green, P., Abrahamson, J., Barlow, A., Daly, M.J., Lincoln, S.E., and Newburg, L. (1987). Mapmaker: An interactive computer package for constructing primary genetic linkage maps of experimental and natural populations. Genomics **1,** 174–181.

Lister, C., and Dean, C. (1993). Recombinant inbred lines for mapping RFLP and phenotypic markers in *Arabidopsis thaliana*. Plant J. **4,** 745–750.

Lynch, M., and Force, A. (2000). The probability of duplicate gene preservation by subfunctionalization. Genetics **154,** 459–473.

Mithen, R., Clarke, J., Lister, C., and Dean, C. (1995). Genetics of aliphatic glucosinolates. III. Side chain structure of aliphatic glucosinolates in *Arabidopsis thaliana*. Heredity **74,** 210–215.

Prescott, A.G. (1993). A dilemma of dioxygenases (or where biochemistry and molecular biology fail to meet). J. Exp. Bot. **44,** 849–861.

Steele, C.L., Crock, J., Bohlmann, J., and Croteau, R. (1998). Sesquiterpene synthases from grand fir (*Abies grandis*): Comparison of constitutive and wound-induced activities, and cDNA isolation, characterization and bacterial expression of delta-selinene synthase and gamma-humulene synthase. J. Biol. Chem. **273,** 2078–2089.

Thies, W. (1979). Detection and utilization of a glucosinolate sulfohydrolase in the edible snail *Helix pomatia*. Naturwissenschaften **66,** 364–365.

Thies, W. (1988). Isolation of sinigrin and glucotropaeolin from cruciferous seeds. Fat Sci. Technol. **8,** 311–314.

Van de Peer, Y., and De Wachter, R. (1994). TREECON for Windows: A software package for the construction and drawing of evolutionary trees for the Microsoft Windows environment. Comput. Appl. Biosci. **10,** 569–570.

Wink, M. (1988). Plant breeding: Importance of plant secondary metabolites for protection against pathogens and herbivores. Theor. Appl. Genet. **75,** 225–233.

Wittstock, U., and Halkier, B.A. (2000). Cytochrome P450 CYP79A2 from *Arabidopsis thaliana* L. catalyzes the conversion of L-phenylalanine to phenylacetaldoxime in the biosynthesis of benzylglucosinolate. J. Biol. Chem. **275,** 14659–14666.

Zrybko, C.L., Fukuda, E.K., and Rosen, R.T. (1997). Determination of glucosinolates in domestic and wild mustard by high-performance liquid chromatography with confirmation by electrospray mass spectrometry and photodiode-array detection. J. Chromatogr. **767,** 43–52.

Gene Duplication in the Diversification of Secondary Metabolism: Tandem 2-Oxoglutarate–Dependent Dioxygenases Control Glucosinolate Biosynthesis in Arabidopsis

Daniel J. Kliebenstein, Virginia M. Lambrix, Michael Reichelt, Jonathan Gershenzon and Thomas Mitchell-Olds

This information is current as of November 26, 2020